

²⁰ Lange and Wacke, "Test report on three- and six-component measurements on a series of tapered wings of small aspect ratio," NACA TM 1176 (May 1948).

²¹ Shanks, R. E., "Low-subsonic measurements of static and dynamic stability derivatives of six flat-plate wings having leading-edge sweep angles of 70° to 84°," NASA TN D-1822 (July 1963).

²² Fournier, P. G., "Wind-tunnel investigation of the aerodynamic characteristics in pitch and sidlip at high subsonic speeds of a wing-fuselage combination having a triangular wing of aspect ratio 4," NACA RM L53G14A (1953).

²³ Unpublished data, Lockheed Supersonic Transport Configuration (1965).

²⁴ Llewellyn, C. P. and Wolhart, W. D., "Effect of Reynolds number on the lateral-stability derivatives at low speed of swept-back- and delta-wing-fuselage combinations oscillating in yaw," NASA TN D-398 (August 1960).

A Useful Method of Airfoil Stall Prediction

DAVID NORRIS REILLY*

Ewing Technical Design, Inc., Philadelphia, Pa.

Introduction

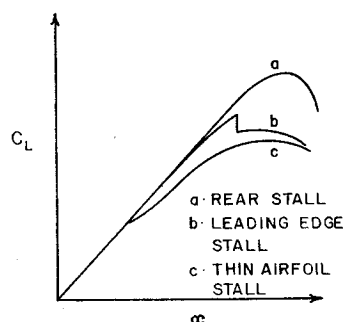
SYSTEMATIC investigations of airfoil stalling characteristics and their relation to the state of the boundary layer began with B. Melville Jones in the mid 1930's. Jones^{1,2} made what is probably the first generalization of stalling characteristics by classifying them into three types: a trailing-edge stall and two types of leading-edge stall. He postulated that stall could result from flow separation at the leading edge as well as the trailing edge, and observed the now well-known "bubble" or localized laminar flow separation.

Subsequent investigators explored the boundary layer and systematically varied the many parameters influencing the mechanism of transition and separation until the three principal types of stall, for which typical lift curves appear in Fig. 1, are now widely accepted: 1) trailing-edge stall, where there is a gradual loss of lift at high lift coefficient as the turbulent separation point moves forward from the trailing edge; 2) leading-edge stall, where there is an abrupt loss of lift, as the angle of attack for maximum lift is exceeded, with little or no rounding over of the lift curves; 3) thin-airfoil stall, where there is a gradual loss of lift at low lift coefficients as the turbulent reattachment point moves rearward.

Types of Stall

The top curve of Fig. 1 represents the lift variation on a typical rear-stalling airfoil. The Reynolds number is high

Fig. 1 Typical stalling curves.



enough that transition from a laminar to a turbulent boundary layer occurs before laminar separation can occur. Crabtree^{3,4} has given, as an empirical condition for such a flow to exist, that the Reynolds number based upon the boundary-layer displacement thickness at separation be greater than 2700, $(R_{\delta^*})_s > 2700$. The first separation of the flow is then a turbulent one somewhere on the rear of the section.

The flows associated with leading-edge stall and thin-airfoil stall are characterized by the accompanying bubble, and typical lift curves appear as the center and lower curves, respectively, of Fig. 1. The laminar-separation bubble is characterized by a tangential separation from the airfoil surface with transition at maximum bubble height and the resulting turbulence spreading so that the flow reattaches. The velocity profiles in the separated layer up to transition are characteristic of those for laminar flow. Further downstream they are distorted by the transition process, and shortly after reattachment the profiles are typical of turbulent boundary layers. The static pressure within the bubble is nearly constant from the point of separation to the point of transition and then increases rapidly to the point of reattachment.

Owen and Klanfer⁵ have classified bubbles as short if their length is of the order of 100 displacement thicknesses at separation, and long if their length is of the order of 10,000 displacement thicknesses at separation. They also determined a displacement thickness Reynolds number below which only long bubbles form and above which only short bubbles form. This value is between 400 and 500. Crabtree⁶ more specifically has found the critical value to be between 400 and 450 when the calculation is based upon experimental pressure distributions and between 450 and 550 when based upon theoretical pressure distribution of potential flow.

The short bubble has a small effect on the over-all pressure distribution, and therefore lift and drag, as long as it reattaches. The long bubble, however, causes a collapse of the leading-edge suction with corresponding loss of lift and increase of drag.

Several criteria exist for the prediction of the laminar separation point. Curle and Skan suggest a form parameter $H = \delta^*/\theta$, where θ is the boundary-layer momentum thickness, exceeding 3.55.

Crabtree observed that there cannot be laminar reattachment at the rear of a bubble. There must be a considerable widening of the streamlines over the rear portion, and this necessitates a turbulent process. There are two principal mechanisms by which transition can occur in the boundary layer.

Tollmien-Schlichting waves are small, regular oscillations in the laminar boundary layer, not associated with freestream turbulence. These waves can amplify at their natural frequency of oscillation resulting in widespread turbulence. Schubauer and Skramstad⁷ have determined a Reynolds number below which the boundary layer is stable for regular disturbances of any wave number.

Turbulent spots occur in a random manner near the upstream limit of the transition region. They spread laterally as wedges and are swept downstream at a velocity less than freestream. New spots are prevented from forming in the downstream region by the enhanced stability of the fluid between the growing turbulent wedges.

The turbulent spot process occurs only when $(R_{\delta^*})_s$ is greater than about 450 and takes place in a lesser length than that for amplification of waves. This has led to the general opinion that transition by the growth of turbulent spots occurs on short bubbles. On long bubbles $(R_{\delta^*})_s$ is usually less than 450, and they will not, in general, support the turbulent spot process. Transition is due to amplification of Tollmien-Schlichting waves.

The exact process and parameters involved in the breakdown of short bubbles are still a matter of some controversy, but it is generally agreed that there are two mechanisms for the process. Crabtree has postulated that bursting will occur

Vibration Analysis of Complex Structures Consisting of Many Members

HELMUT FALKENHEINER*
 Vereinigte Flugtechnische Werke,
 München, West Germany

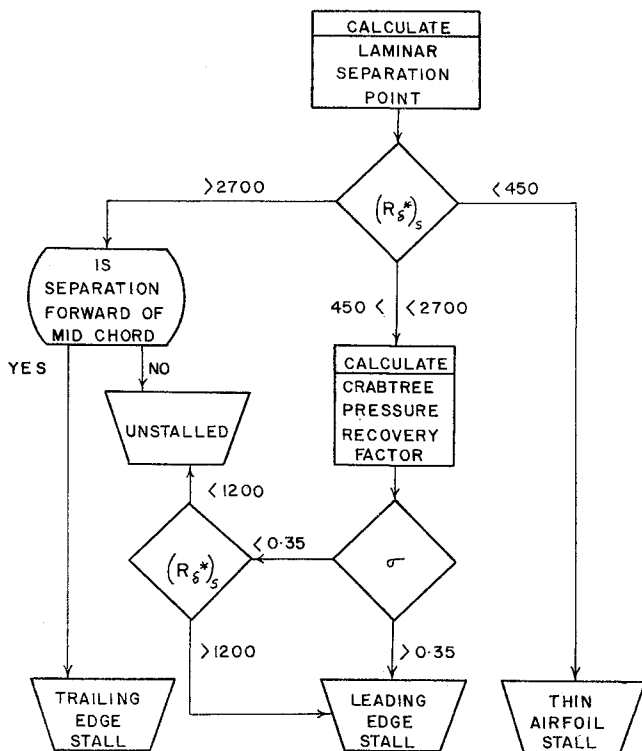


Fig. 2 Stall prediction scheme.

when the maximum shear stress that can be tolerated by the reattaching turbulent boundary layer is exceeded and has derived a pressure recovery factor.

$$\sigma = \frac{(C_p)_{\text{transition}} - (C_p)_{\text{separation}}}{1 - (C_p)_{\text{separation}}}$$

to represent this stress. Experimental investigations have determined $\sigma = 0.35$ to be the limiting value above which the bubble bursts suddenly and the flow breaks down into the pattern associated with fully separated flows. An alternate cause of short-bubble breakdown is a turbulent separation immediately downstream of reattachment. This is referred to as re-separation and only occurs when $(R\delta^*)_s > 1200$.

Summary

Some of the mechanism of airfoil stall have been discussed and parameters easily measured experimentally or calculated by most numerical solutions of boundary-layer equations selected to predict stalling behavior. Figure 2 summarizes the procedures outlined in this note and should be easily incorporated into existing airfoil analysis methods.

References

- 1 Jones, B. M., "An experimental study of the stalling of wings," British Aeronautical Research Council R & M 1588 (1933).
- 2 Jones, B. M., "Stalling," J. Roy. Aeron. Soc. **38**, 753-770 (1934).
- 3 Crabtree, L. F., "Effects of leading edge separation on thin wings in two-dimensional incompressible flow," J. Aeronaut. Sci. **24**, 507-604 (1957).
- 4 Crabtree, L. F., "Prediction of transition in the boundary layer on an aerofoil," J. Roy. Aeron. Soc. **62**, 525-528 (1958).
- 5 Owen, P. R. and Klanfer, L., "On the laminar boundary layer separation from the leading edge of a thin aerofoil," Royal Aeronautical Establishment Rept. Aero. 2508 (October 1953).
- 6 Crabtree, L. F., "The formation of regions of separated flow on wing surfaces. Part II, laminar separation bubbles and the mechanism of leading edge stall," Royal Aeronautical Establishment Rept. Aero. 2578 (1959).
- 7 Schubauer, G. B. and Skramstad, H. K., "Laminar boundary layer oscillations and transition on a flat plate," NACA Rept. 909 (1943).

LINEAR elastic properties of complex aircraft and spacecraft structures consisting of many members are commonly represented by the stiffness influence coefficients matrix. In vibration analysis of such structures, this matrix is used for both the "lumped masses" and the "assumed modes" methods, although the latter may be adapted to continuous media. However, the stiffness influence coefficients matrix represents not only a numerical evaluation of complicated stress-strain integrals but also a very rigid procedure for discretizing continuum properties. It leads to very high order matrices if calculations are intended beyond the first few natural frequencies and mode shapes of a structure. Experience shows that the discrepancy between the necessary order of the matrices and the actually calculable number of eigenvalues increases sharply and the scope of work becomes excessive, even with advanced computer facilities. This may be attributed to the rapid degeneration of the stiffness influence coefficients matrix as its reference points converge, yielding to the stiffness influence function [see, e.g., Eq. (27), Ref. 2, which represents the divergent development for the stiffness influence function in series of eigenfunctions]. Thus, the stiffness influence coefficients matrix seems to be a barrier to more refined vibration calculations for continuous but complex systems, where also the well-known straightforward differential or integral equation methods fail due to inextricable boundary conditions or kernel functions, respectively.

In an effort to avoid both the difficulties of boundary conditions and kernel functions, and the uncertainties of higher-order stiffness influence coefficients matrices, a "direct method" procedure was developed to compute the generalized stiffness matrix directly from the design data of the structure as part of the assumed modes method.¹ A set of assumed modes $\mathcal{F}_r(x,y,z)$; $r, s = 1, 2, 3, \dots, r$ (where the number r is at most two or three times the number of eigenmodes sought) is chosen to satisfy the conditions of the Rayleigh-Ritz method and some essential conditions of the Galerkin application. This means that the modes are roughly the same as those commonly used, chosen from previous analysis of similar structures, from exact solutions of neighboring systems, etc., but completed more or less intuitively in details. With these modes the elements ϕ_{rs} of the generalized stiffness matrix are computed by formula, as shown in the example, where they are written out in three-dimensional Cartesian coordinates.

The assumed modes need not be given analytically. The numerical evaluation of the integrals is programmed for the computer, which finally delivers the complete matrix ϕ , and, as a sort of by-product, the generalized mass matrix M . Each generalized stiffness element requires approximately the same amount of computer time as one element of a stiffness influence coefficient matrix, but there is a relatively small number, r^2 , of these generalized stiffness elements to be computed. The generalized stiffness elements are built up of solely additive parts. Each part is computed separately and concerns a well-defined part of the strain energy of a structural element. In this way it is relatively easy to

Received October 10, 1966; revision received August 17, 1967. The author wishes to thank I. Soukhanov for his help in translating the manuscript.

* Head of the Hauptabteilung Aerolastik.

[6.02]